Flexural behavior and finite element analysis of waste tires steel fiber reinforced concrete beams with basalt reinforcement

Teng Ge[1], *Tianfu* Liang[2,*], and *Xiaochun* Fan[1]

[1]School of Civil Engineering and Architecture, Wuhan University of Technology, Hubei Wuhan 430070, China
[2]Wuhan Metro Group Co., Ltd , Hubei Wuhan 430000, China

Abstract. Waste Tire Steel Fiber(WTSF) was used in different proportions (0%, 0.5%).1% and 1.5%) were mixed with ordinary concrete to produce WTSF reinforced concrete. Based on basalt fiber reinforced polymer and WTSF concrete, a new structural system, WTSF concrete beam with basalt reinforcement, is proposed. On the basis of the theory test, using the ABAQUS finite element software to simulate basalt rebar waste of the bending properties of steel fiber concrete beam, to obtain the stress nephogram, cracking load, ultimate bearing capacity, load deflection curves and crack location map, comparative tests and fitting results show that WTSF volume content 0% less muscle damage, 0.5% for balance, 1% and 1.5% are superreinforced failure. With the increase of WTSF content, both cracking load and ultimate bearing capacity are improved. Meanwhile, theoretical calculation formulas of relevant components are given to guide engineering practice.

1 Foreword

In recent years, many experts at home and abroad have made many tests on the bending performance of the reinforced concrete beam of various materials. Ordinary reinforced concrete beam is the most widely used, this is due to its convenient construction, easy to form, but into the 21st century, with the progress of science and technology, in prefabricated structure, bridge engineering, military protection engineering and nuclear reactor containment requirements for concrete, ordinary reinforced concrete low tensile strength, poor ductility, easy to crack, steel corrosion and other shortcomings can not meet its engineering requirements, so many scholars put forward fiber reinforced fiber reinforced composite(Fiber Reinforced Polymer, FRP)[1-2].

Basalt fiber reinforced polymer (BFRP bars) is a variety of fiber reinforced polymer reinforcement formed by crushing basalt ore as the basic material, adding it to the furnace, melting at high temperature, stretching and extrusion. It has the advantages of not easy corrosion, light weight, high strength, fatigue resistance It has many advantages, such as thermal insulation, electromagnetic neutrality and so on, so it has prominent application

* Corresponding author: liangtf@wuhanrt.com

prospects in the field of engineering construction[3-4].Zhu S T[5] carried out bending tests on five BFRP bars reinforced concrete beams by changing concrete strength and BFRP bars reinforcement ratio. The strain changes of concrete and BFRP bars reinforcement in the beam span under different loads are analyzed, and the calculation formulas of cracking moment, crack width, ultimate bearing capacity and deflection of the new system beam are put forward. Lapko[6] carried out bending test on BFRP bars reinforced concrete beam, mainly studied its deformation capacity, and pointed out that there will be a slight deviation between the deflection obtained by previous theoretical calculation and the test results. Through the research of these scholars, we can see that the bearing function of BFRP bars reinforcement concrete beam is greater than ordinary concrete. Whether BFRP bars reinforcement can replace ordinary reinforcement applied in large practical engineering needs to conduct a lot of test verification, but the test cost too much money and manpower, and it becomes extremely important to analyze the performance of the finite element software modeling such as ABAQUS.

Nevertheless, due to the low elastic modulus of BFRP bars reinforcement, its members have problems such as large deformation and wide crack in the process of use[7-8]. Through the test, scholars at home and abroad generally agree that the thing added of industrial steel fiber (ISF) can efficiently reduce the disadvantages such as large mid span deflection of concrete beam[9], wide concrete crack in tensile area , and greatly improve the strength and toughness of concrete[10-11]. However, in practical engineering, the examples of transporting industrial steel fiber are very limited, because industrial steel fiber is more expensive and environmentally friendly. Therefore, some scholars put forward the idea of adding WTSF recovered from waste tires into concrete to replace ISF[12-14], which not only reduces the use cost, but also alleviates the "black pollution" environmental pollution caused by waste tires and the energy consumption of industrial steel fiber[15-17]. Considering comprehensively, using WTSF as the fiber source of fiber reinforced concrete is a more ideal choice[18]. However, there are few reports on the effect of WTSF instead of ISF on the flexural behavior of BFRP bars reinforced concrete beams.

Therefore, in this paper, WTSF is used to replace ISF, and the waste steel fiber reinforced concrete is combined with BFRP bars to form WTSF reinforced concrete beams with BFRP bars. Based on the trial results, the simulation calculation of four bending test by ABAQUS finite element analysis software, verified the reliability of the WTSF reinforced concrete beams with BFRP bars, laying the theoretical foundation for the engineering application of the WTSF reinforced concrete beams with BFRP bars.

2 Test Overview

2.1 Mix ratio of raw materials and concrete

Cement with P·O 42.5 specified in GB 175-2007 General Portland Cement; coarse aggregate with gravel with good grading of less than 1% and particle size of 5~20 mm; fine aggregate with 1510 kg/m^3 accumulation density, apparent density of 2500 kg/m^3 and fine modulus of 2.8;WTSF extracted from recycled waste tires by Shanghai Jinghan Company. The apparent shape and length distribution are shown in Fig. 1; mechanical and physical properties are shown in Tab. 1.Water reducing agent is polycarboxylic acid water reducer, water reduction rate is more than 25%; the HPB300 type steel bars with 6mm diameter are used for the erecting and stirrups, and the BFRP bars with 8mm diameter are used for the deep spiral basalt bars. The related properties of the reinforcement are given in Tab. 2.

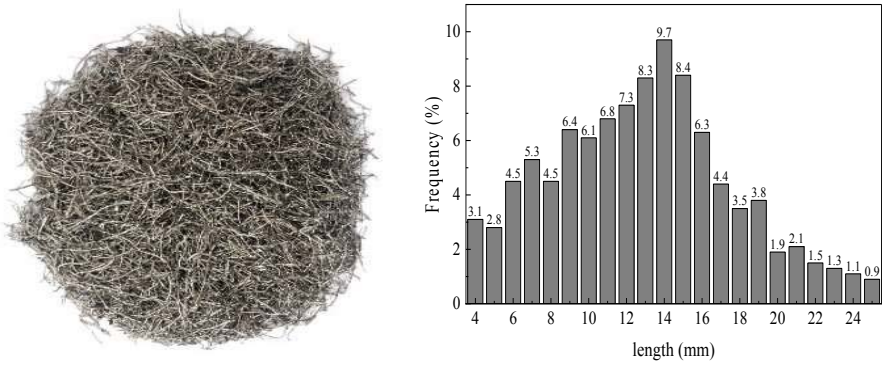

(a) Physical drawing (b) Length distribution frequency diagram

Fig. 1 WTSF

Tab. 1. Physical and mechanical properties of WTSF

Fiber morphology	Length/mm	Diameter/mm	Tensile Strength/MPa	Elastic Modulus/GPa
	4~25	0.22	2165	200

Tab. 2. Mechanical Properties of rebar

Model	Diameter/mm	Yield strength/MPa	Tensile Strength/MPa	Elastic Modulus/GPa
HPB300	6	320.0	465	202
BFRP bars-8	7.20	\	1394	58.2

Referring to the study of domestic and foreign scholars on WTSF volume incorporation, the volume incorporation of WTSF incorporated in the concrete matrix was set to 0%, 0.5%, 1.0% and 1.5%[12,15]. The concrete mix ratio is shown in Tab. 3.

Tab. 3. Mix proportion of the concrete (kg/m^3)

Cement	Sand	Stone	Water	Water reducing agent
477	485	1283	200	4.0

2.2 Testing program

For purpose of ensuring the dependability of the test, two test beams are set for each group. The size and reinforcement of the test specimen are designed according to the relevant technical regulations of China, and the size of the test beam is 120 mm×200 mm×2000 mm, the length of longitudinal reinforcement is 1980 mm, the thickness of concrete cover is 20 mm, and the calculation span of beam is 1800 mm. BFRP bars with a diameter of 8 mm is

selected as the tensile longitudinal reinforcement, HPB300 reinforcement with a diameter of 6 mm is selected as the erection reinforcement and stirrup, and the stirrup spacing is 100 mm. Stirrups are not conFig.d in the pure bending section. The specific design parameters are shown in Tab. 4, and the reinforcement diagram of WTSF concrete beam with BFRP bars is shown in Fig. 2.

Tab. 4. Main design parameters of test beam

Number	Longitudinal tendon	Volume content of WTSF/%	Stirrup
B8R00-1, 2	2B8	0	A8@100
B8R05-1, 2	2B8	0.5	A8@100
B8R10-1, 2	2B8	1.0	A8@100
B8R15-1, 2	2B8	1.5	A8@100

Note: B8R05-2 indicates two BFRP bars of 8mm diameter, and the volume of scrap steel fiber is 0.5%, which is the No. 2 Beam in reorganization.

The test is according to GB/T 50152-2012 Standard for Concrete Structure, and the test beam is loaded by four-point bending and 500kN press for loading equipment,as shown in Fig. 3.The loading method adopts preloading and formal loading, and the maximum preload is set as 50% of the estimated cracking load of the test beam. The load is loaded twice to debug the loading device and measurement equipment. After confirming that there is no abnormality, the load is unloaded to zero.Formal loading adopts graded loading with a loading step distance of 5kN. When the estimated cracking load value is approached, level 0.5kN is changed until the test beam is crushed, and various test data are collected after each stage load holds 5 min, the field loading of the test beam is shown in Fig. 4.

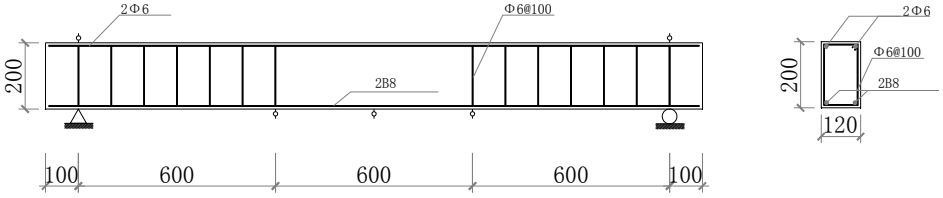

Fig. 2 Reinforcement diagram of WTSF concrete beam with BFRP bars

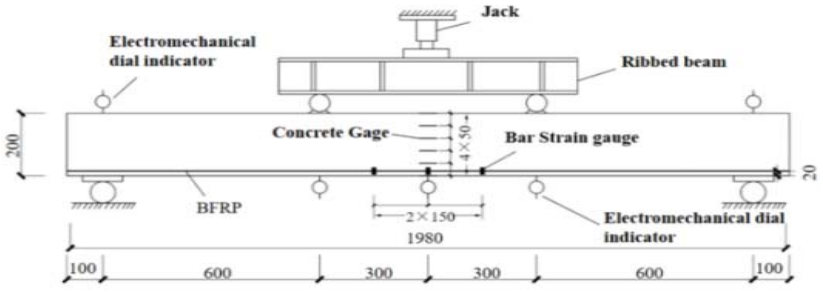

Fig. 3 Loading device on measuring points(mm)

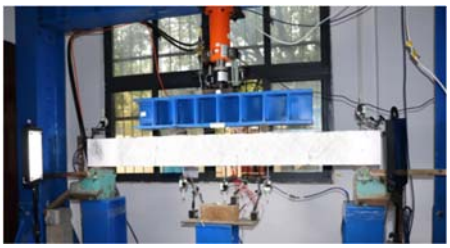

Fig. 4 Field loading experiment diagram

2.3 Test results

The test results of 28 days of cube compression, split tensile and elastic modulus and WTSF reinforced concrete beams with BFRP bars are shown in Tab. 5.

Tab. 5. Test result

Number	f_{cu} /MPa	f_c /MPa	f_{ts} /MPa	E_C /GPa	Average cracking load/kN	Ultimate load/kN
R00	40.00	35.2	3.52	32.6	8.32	58.76
R05	49.53	39.1	3.86	34.5	9.76	61.24
R10	50.92	40.2	4.34	34.7	10.26	52.21
R15	51.44	40.7	4.83	34.9	11.85	66.53

Note: f_{cu} is cube compressive strength, f_c is axial compressive strength, f_{ts} is splitting tensile strength, and E_C is elastic modulus.

3 Finite Element Analysis

3.1 Selection of the cell type

WTSF concrete beam with BFRP bars has concrete units, BFRP bars unit, standing tendon and stirrup unit, fiber units, the concrete unit should be simulated by solid unit, because the solid unit can reflect the volume characteristics of geometry, there are many types of entity unit in ABAQUS software, for the accuracy of model calculation and sand leakage control three eight node reduce integral solid unit C3D8R, this unit can alleviate the unit too rigid or small deflection, can also avoid shear lock or volume lock[19]; In order to run simple calculation, for BFRP bars units, the reinforcement and stirrup unit and fiber unit do not consider bending, do not bear the bending moment, and the 3D two-dimensional truss unit T3D2 is uniformly adopted. The established model is shown in Fig. 5:

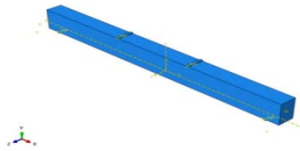

(a) Model drawing of test beam

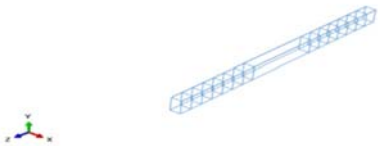

(b) Reinforcement cage framework model drawing

(c) 1% steel fiber model

(d) Detailed enlarged drawing of steel fiber model

Fig. 5 Concrete model drawing

3.2 Material constitutive model

The material constitutive model in this paper is divided into constitutive model of concrete, constitutive model of fiber, constitutive model of BFRP bars, auxiliary steel bars and stirrup configuration model. The constitutive model of concrete is the most important constitutive model, which greatly determines the results of the simulation. In order to comprehensively analyze the behavior of crushing or cracking of concrete, the concrete plastic damage model, referred to as CDP, which can well simulate the brittle characteristics of concrete. This paper adopts the damage constitutive model mentioned in GB50010-2010, and the compression stress and strain relationship of WTSF concrete when ignoring the influence of bond slip and standing reinforcement is shown in formula (1).

$$\sigma_c = \begin{cases} f_c\left[1-\left(1-\frac{\varepsilon_c}{\varepsilon_0}\right)^2\right] & \varepsilon_c \le \varepsilon_0 \\ f_c & \varepsilon_0 \le \varepsilon_c \le \varepsilon_{cu} \end{cases} \tag{1}$$

σ_c is the compressive stress of concrete, unit: MPa; f_c is the axial compressive strength of concrete, unit: MPa; ε_0 is compressive strain of concrete; Is the compressive strain of WTSF concrete when it reaches f_c , calculated according to formula (2), ε_{cu} is the ultimate compressive strain of concrete, which is taken as 0.0045 according to the test results.

$$\varepsilon_0 = 0.0007 V_{rsf} \frac{l_{rsf}}{d_{rsf}} + V_{rsf} 0.0021 \tag{2}$$

V_{rsf} is the volume content of WTSF; $\frac{l_{rsf}}{d_{rsf}}$ is the length diameter ratio of WTSF

In order to give its model with good yield strength and flow criteria, the parameters selected by its CDP model are shown in Tab. 6[20]:

Tab. 6. CDP parameters of WTSF reinforced concrete beams with BFRP bars

Eccentricity	ω/°	f_{b0}/f_{c0}	Kc	Elastic modulus/GPa	Poisson's ratio	Viscosity parameter
0.1	30	0.22	0.667	32.6	0.2	1E-05

Note: ω represents the expansion angle, f_{b0}/f_{c0} represents the stress ratio, and K_C is the shape factor.

For the erection reinforcement and stirrup are ordinary reinforcement with the model of HPB300, the ideal elastic-plastic model should be adopted, and its constitutive model is shown in Fig. 6a; In order to calculate the convergence, WTSF can be simply regarded as a complete linear elastic relationship without yield stage[21]; BFRP bars maintains linearity from tension to failure, and there is no obvious yield stage. Its constitutive model is similar to that of fiber. See Fig. 6b for this composition.

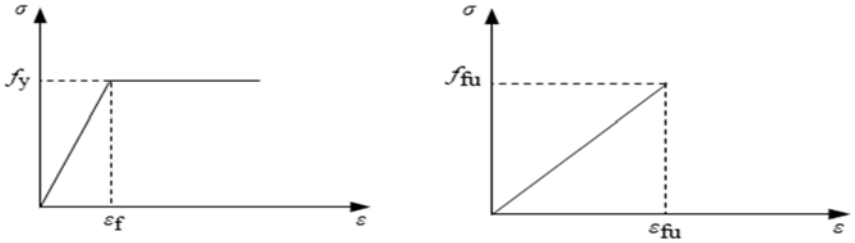

(a) HPB300 (b) BFRP bars

Fig. 6 Constitutive model of reinforcement

3.3 Grid division

The ABAQUS finite element software provides many tools to divide the grids, such as grid seed tools, segmentation tools, virtual topology tools, network editing tools, etc. To obtain high-quality grids and improve the efficiency of partition grids, we apply the grid seed tool.The size of the grid directly determines the accuracy of the computation, but the results are not easy to converge if the grid is too small. If you can simply divide the entire component into grids of uniform size, but this will greatly increase the computation time. To improve analysis accuracy and reduce model size and shorten computation time, grids should be refined at important sites and thicker grids at other unimportant sites. Important sites can be predicted by test, such as areas of stress concentration and areas with large plastic strain. In this paper, 20 mm grid is selected in the middle of the two beams, and 50 mm grid is used in the part and cushion outside the two supports, with good simulation effect.

3.4 Boundary conditions and load application

In order to avoid the nonconvergence of the model due to local stress concentration, the rigid pad is set at the load point and support, the beam body and the surface of the rigid pad to prevent the pad from flying out of the model under eccentric force, set the reference coupling on the pad surface, and then control the degrees of freedom of U1, U2 and UR3 at the reference point to realize the boundary conditions of the hinge support. The simulation process adopts the displacement loading mode, the displacement is set at the reference point at the center of the surface on the pad, through the data of the test to make the appropriate displacement completely destroy the test piece. To calculate better convergence, assuming the relative slip between bars and concrete, the reinforcement cage was embedded in concrete using Embedded Region.

3.5 Comparative analysis of the destruction patterns

Fig. 7 shows the stress cloud map of concrete and reinforcement skeleton in the finite element simulation of each group of test beams. In the Fig., when the concrete in the compression area or BFRP bars at the bottom reaches the ultimate stress, it indicates that the test beam has

compression failure or tensile failure.

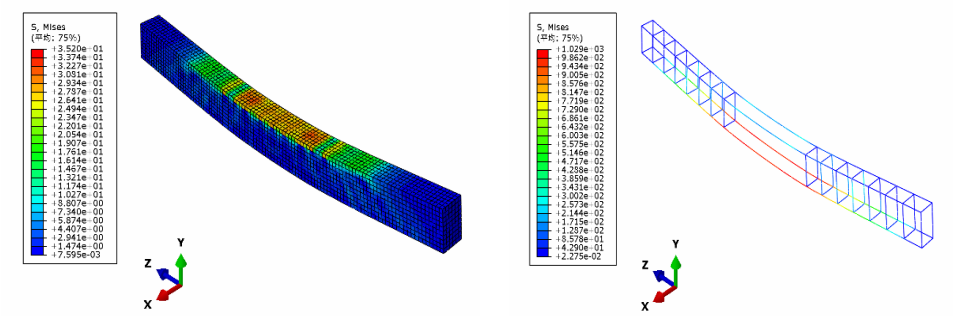

Concrete Stress (MPa) Reinforcement skeleton stress(MPa)

(a) B8R00

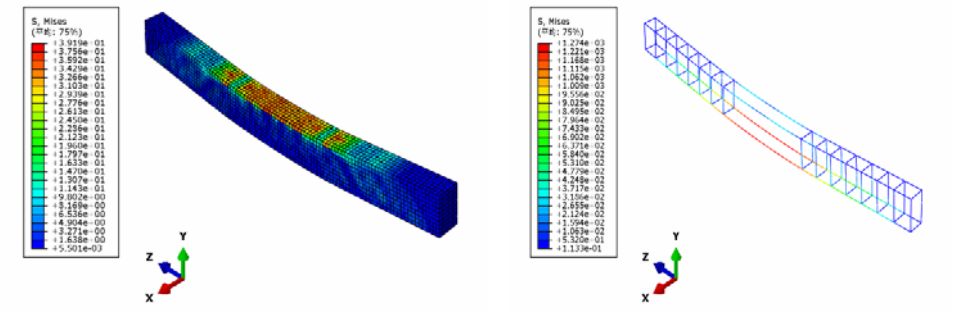

Concrete Stress(MPa) Reinforcement skeleton stress(MPa)

(b) B8R05

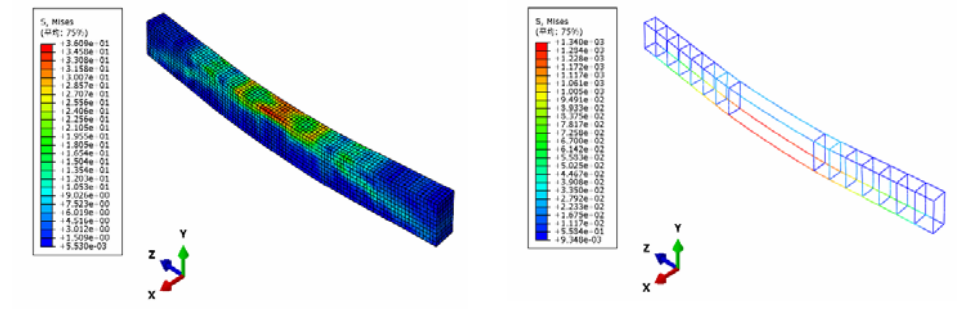

Concrete Stress(MPa) Reinforcement skeleton stress(MPa)

(c) B8R10

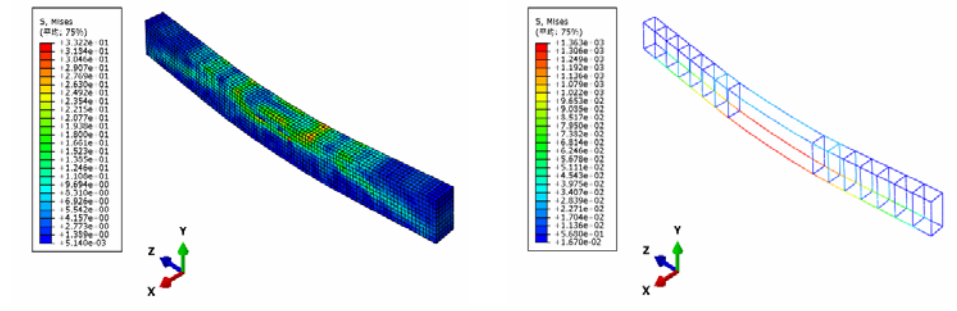

Concrete Stress(MPa) Reinforcement skeleton stress(MPa)

(d) B8R15

Fig. 7 Stress nephogram of test beam

According to the stress cloud chart in Fig. 7, the concrete in the compression area of B8R00 reaches the ultimate strain and the maximum stress of the lower end reaches 1024 MPa, in the compression area of B8R05, the maximum stress of the lower area reaches 1274 MPa, which is the balance failure when the reinforcement and B8R10 reach 1300 MPa. In the Fig., when the concrete in the compression area or BFRP bars at the bottom reaches the ultimate stress, it indicates that the test beam has compression failure or tensile failure. By comparing with the experimental phenomena, it is found that the failure mode of ABAQUS finite element simulation model is highly consistent with that of the actual test components.

3.6 Cracking load and limit bearing capacity comparison

The ABAQUS simulation value and test value of the cracking load and limit load capacity of the test beam are shown in Tab. 7. As shown from the Tab. 7: the test beam cracking load and limit bearing capacity obtained by finite element simulation are close to the test value, and the mean and standard deviation of each test beam cracking load simulation value and test value ratio are 1.07 and 0.03 separately; the mean and standard deviation of limit bearing capacity simulation value and test value ratio are 1.03 and 0.01 separately. Finite element simulation beam limit bearing capacity is slightly greater than the test value, the reason is that ABAQUS software simulation, components as ideal and identical, WTSF as elastic material and WTSF is not connected with each other, independent in space, and test beam in actual pouring artificial error, vibration, maintenance and other factors will lead to the test beam concrete strength failed to target strength, gravity and vibration may also steel fiber settlement or handover together, leading to anisotropy of concrete mechanical properties. Meanwhile, the boundary conditions and constraints of the test beam without considering the sliding influence between reinforcement and concrete.

Tab. 7. Comparison of simulated and experimental values

Number	Simulated value of F_{cr}/kN	Test value of F_{cr}/kN	Simulation value of F_u/kN	Test value of F_u/kN	S/T	
					F_{cr}	F_u
B8R00	8.98	8.29	60.18	58.77	1.08	1.02
B8R05	10.62	9.76	62.65	61.14	1.09	1.02
B8R10	11.03	10.26	64.76	62.21	1.08	1.04
B8R15	12.17	11.85	68.98	66.53	1.03	1.04
Average value	/	/	/	/	1.07	1.03
Standard deviation	/	/	/	/	0.03	0.01

3.7 Comparison of load-deflection curves

The simulation results of test beam load-deflection curve are shown in Fig. 8. In the light of the Fig. 8, the load-deflection curve of the test beam simulated by ABAQUS is basically

consistent with the load-deflection curve of the test beam. The load-deflection curve obtained from the simulation is roughly two sections, with the component cracking as the dividing point. Before the component cracks, the simulation value is close to the test value and the two curves basically overlap. When the member cracks, the simulation degree curve is slightly higher than the test results, and the midspan deflection of the simulated test beam is slightly less than the test value under the same load. The test beam load-deflection curve simulation results exist slightly wrong, because the relative sliding between BFRP bars and concrete is not considered during the finite element simulation.

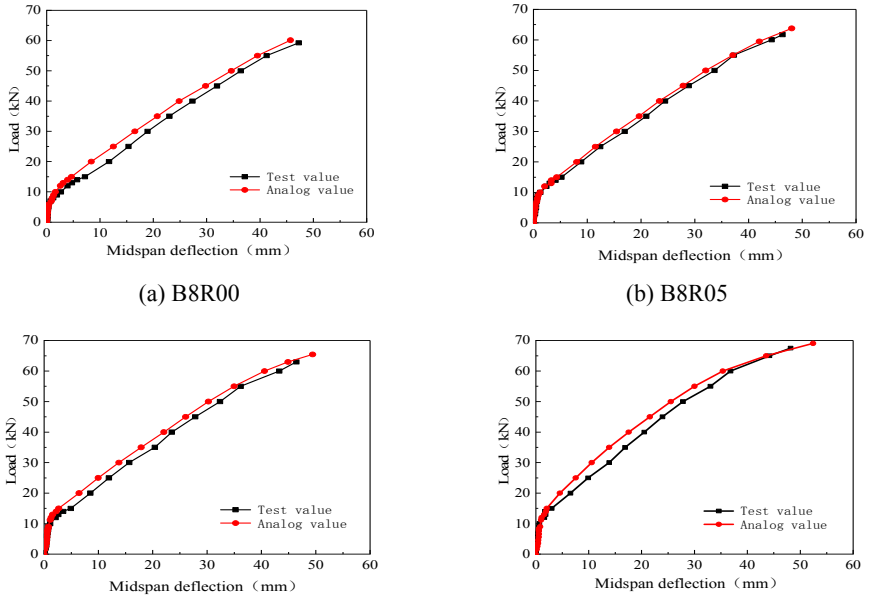

(a) B8R00 (b) B8R05

(c) B8R10 (d) B8R15

Fig. 8 Comparison of load deflection curves of test beams

4 Conclusion

The WTSF concrete was prepared with the total content of WTSF of 0%, 0.5%, 1% and 1.5%. On the basis of experiment, the bending test of four WTSF reinforced concrete beams with BFRP bars is simulated and calculated with ABAQUS finite element software, and its mechanical properties under different WTSF content are analyzed. The following main conclusions are drawn:

(1) The test beam with 0% WTSF content belongs to tensile failure, the test beam with 0.5% WTSF content belongs to equilibrium failure, and the test beam with 1% and 1.5% WTSF content belongs to compression failure. With the increase of WTSF volume content, the post cracking stiffness of the test beam gradually increases. The results of finite element simulation completely accord with the experimental phenomenon.

(2) The model calculation results simulated by ABAQUS are consistent with the test results in terms of failure mode, cracking load, ultimate bearing capacity load, load deflection curve, crack development and calculation formula. Both verify the accuracy of the results. It shows that ABAQUS finite element model can accurately predict the bending test of basalt reinforced WTSF reinforced concrete beams.

(3) According to the simulation results, the cracking load and ultimate load of basalt

reinforced WTSF concrete with 1.5% WTSF are 1.36 times and 1.14 times that of basalt reinforced concrete without WTSF. We can draw that with the increase of the content of WTSF, the cracking load and ultimate load gradually increase.

(4) There is a gap between the bond theory of BFRP bars reinforced concrete and that of ordinary reinforcement and concrete. This simulation simply believes that the two are useless, and the relative slip is one of the reasons why the results are not completely consistent with the actual results.

References

1. Atutis M, Valivonis J, Atutis E. Experimental study of concrete beams prestressed with basalt fiber reinforced polymers. Part I: Flexural behavior and serviceability[J]. Composite Structures, 2018, 183:114-123.
2. ZHANG W X, HU B B, WANG G J, et al.Research progress and improvement of constitutive model for bonding properties of FRP bars to concrete [J]. Chinese Journal of Civil and Environmental Engineering, 202:1-12. (in Chinese)
3. ZHU H T, CHENG S Z, GAO D Y, et al.Experimental and theoretical study on bending capacity of steel fiber high strength concrete beams with BFRP bars [J]. Acta Materiae Compositae Sinica,2018,35(12):3313-3323.
4. KONG X Q, YU Y, XING L L, et al.Experimental Study on the Flexural Behavior of Concrete Beams Mixed with BFRP bars and Reinforcement [J]. Fiber Reinforced Plastics/Composites,2018,(8):48-54.
5. ZHU S T. Experimental Research on the Flexural Behavior of Basalt Reinforced Concrete Beams [D]. Mianyang: Southwest University of Science and Technology, 2016.
6. Lapko A, Urbanski M. Experimental and theoretical analysis of deflections of concrete beams reinforced with basalt rebar[J]. ARCHIVES OF CIVIL AND MECHANICAL ENGINEERING, 2015,15(1):223-230.
7. LIU Y, GU Q, TIAN S, et al.Experimental Study on Fatigue Behavior of Steel Fiber Reinforced Concrete [J]. Bulletin of the Chinese Ceramic Society,2019,38(5):1356-1361,1368.
8. CHENG S Z, ZHU H T, WANG R L, et al.Journal of Civil Engineering and Management, 2017, 34(2):87-90,94.
9. Yang J-M, Min K-H, Shin H-O, et al. Effect of steel and synthetic fibers on flexural behavior of high-strength concrete beams reinforced with FRP bars[J]. Composites Part B: Engineering, 2012, 43(3):1077-1086.
10. Abed F, Alhafiz A R. Effect of basalt fibers on the flexural behavior of concrete beams reinforced with BFRP bars[J]. Composite Structures, 2019, 215:23-34.
11. Vakili S E, Homami P, Esfahani M R. Effect of fibers and hybrid fibers on the shear strength of lightweight concrete beams reinforced with GFRP bars[J]. Structures, 2019, 20:290-297.
12. FAN X C, XIONG L F, WANG P. Experimental and theoretical calculation of bias pressure of basaltic reinforced steel fiber reinforced concrete short column [J]. Bulletin of the Chinese Ceramic Society, 2020,39(10):3161-3168.
13. Al-Musawi H, Figueiredo F P, Bernal S A, et al. Performance of rapid hardening recycled clean steel fibre materials[J]. Construction and Building Materials, 2019, 195:483-496.

14. Grzymski F, Musiał M, Trapko T. Mechanical properties of fibre reinforced concrete with recycled fibres[J]. Construction and Building Materials, 2019, 198:323-331.
15. YANG J, PENG G F, SHUI G S.Mechanical properties of recycled steel fiber reinforced ultra-high performance concrete [J]. Acta Materiae Compositae Sinica, 2019,36(08):1949-1956.
16. Caggiano A, Folino P, Lima C, et al. On the mechanical response of Hybrid Fiber Reinforced Concrete with Recycled and Industrial Steel Fibers[J]. CONSTRUCTION AND BUILDING MATERIALS, 2017,147:286-295.
17. Domski J, Katzer J, Zakrzewski M, et al. Comparison of the mechanical characteristics of engineered and WTSF used as reinforcement for concrete[J]. JOURNAL OF CLEANER PRODUCTION, 2017,158:18-28.
18. Sengul O. Mechanical behavior of concretes containing WTSFs recovered from scrap tires[J]. CONSTRUCTION AND BUILDING MATERIALS, 2016,122:649-658.
19. WANG Q, CHANG K, HOU K K, et al.Concrete Uniaxial Constitutive Model for Abaqus Beam Element [J]. Journal of Building Science and Engineering, 2018,35(05):194-202.
20. ZHANG F, MA J X, NAN Y.Parameter Selection and Validation Calculation of Concrete Plastic Damage Model [J]. Concrete and Cement Products,2021(01):7-11.
21. LI Y, ZHU S, BAI H Y.Simulation and analysis of flexural performance of recycled steel fiber reinforced concrete [J]. Northern Building, 2020,5(04):6-10.

List of nomenclatures

Symbols	Implications
f_{cu}	cube compressive strength
f_c	axial compressive strength
f_{ts}	splitting tensile strength
E_C	elastic modulus
σ_c	the compressive stress of concrete
ε_0	compressive strain of concrete
V_{rsf}	the volume content of WTSF
$\frac{l_{rsf}}{d_{rsf}}$	the length diameter ratio of WTSF
ω	the expansion angle
f_{b0}/f_{c0}	the stress ratio
K_C	the shape factor.
F_{cr}	cracking load
F_u	ultimate load